2021-0180

Heterogeneous Traffic Management using METANET Model with Filtered Feedback Linearization Control Approach

Pouria Karimi Shahri, Amir H. Ghasemi
Department of Mechanical Engineering and Science, University of North Carolina at Charlotte.
Pkarimis@uncc.edu
Ah.ghasemi@uncc.edu

ABSTRACT

This paper presents a Filtered-Feedback-Linearization (FFL) controller for a non-signalized heterogeneous traffic network consisting of human-driven and autonomous vehicles at a macroscopic level. The FFL controller requires limited model information and it is effective for command following and rejection of unknown-and-unmeasured disturbances. This paper distinguishes between human-driven and autonomous vehicles in terms of their operational characteristics and controllability. To describe the traffic network's behavior, we introduce an extended heterogeneous METANET model wherein the traffic flow, density, and velocity dynamics of each vehicle class are described. To develop traffic control policies, we propose a filtered-feedback-linearization control approach wherein the autonomous vehicles and human-driven vehicles are modeled as controllable agents. FFL controller sends the optimal suggested velocity of autonomous vehicles and human-driven vehicles as the controller command to the traffic system to reach the desired velocity, density, and average flow rate of each sub-network. Numerical simulation demonstrates the effectiveness of the proposed approach in managing the traffic flow of a heterogeneous traffic system.

KEYWORDS: Heterogeneous Traffic Network, Autonomous Vehicles, Traffic Control, Filtered Feedback Linearization Control, METANET Model

INTRODUCTION

Traffic jams cost US $87 billion in 2018 [1]. Different control strategies with different traffic flow models have been developed to manage traffic networks [2, 3]. Among these efforts, connected automated vehicle (CAV) technologies have received increasing attention recently [2, 3]. Recent studies have shown the positive impacts of CAVs technology on fuel consumption, reduced travel time, and improved safety [4, 5]. However, for practical purposes, (i) no traffic network in the near future will consist entirely of automated vehicles, and (ii) vehicles (even automated ones, but especially the human-driven ones) will never behave entirely homogeneously. Until then, there exists significant uncertainty in the performance of mixed CAV and human-driven traffic environments [6–8]. Therefore, it is essential to develop control strategies that take into account the uncertainty associated with the heterogeneity in the traffic network and understand the extent to which these strategies improve the performance of the network.

Traffic control and management problem have been studied at both macroscopic and microscopic levels [9–11]. At the microscopic level, the problem focuses on controller synthesis for individual vehicles, where each vehicle evaluates its own control solution with available information to improve its own performance (such as energy consumption or travel time) [12, 13]. However, the egotistical nature (only focusing on its own performance) of this type of controller and availability of only local information can deteriorate the overall traffic network's traffic flow [14]. Macroscopic controllers, on the other hand, focus on improving the aggregated traffic behavior (such as overall traffic flow), but they operate at a lower frequency and cannot evaluate the optimal actions of individual vehicles [15–18]. To leverage the advantages of both macro-level and micro-level controllers, hierarchical control frameworks have been developed, with macroscopic controllers at the high-level and microscopic controllers at the low-level [19, 20].

This paper is focused on developing a set of macroscopic traffic control policies for a non-signalized heterogeneous traffic network. To this end, we model the macroscopic behavior of a heterogeneous traffic network by a multi-class

METANET model. In this model, the density and velocity of each vehicle class are described in the traffic dynamics. The considered freeway METANET model describes the traffic system, which is naturally affected by uncertainties since the mainstream inflow, the traffic demands on the on-ramps, and the flows exiting the off-ramps are not a priory known.There are various extensions to the classic METANET model such as Multi-class METANET Model [21] and Extended METANET model [22]. To manage the congestion in a heterogeneous traffic network, a Filtered Feedback Linearization control is proposed. In this problem, we assume that we have a hierarchical control structure in the traffic system. The higher-level controller determines the desired densities of each vehicle class in each sub-network according to the cost function of the whole traffic system (Reducing TTT, reducing energy consumption, increasing the average flow rate, etc.). At the lower level, the controller determines the suggested velocity of each vehicle class reach to the desired densities in the sub-network. We employed Filtered Feedback linearization (FFL) control to determine the suggested velocity for each class of vehicles so that the desired density determined in the upper level can be achieved. FFL is a high-parameter-stabilizing control technique that addresses both command following and disturbance rejection for multi-input-multi-output nonlinear systems where the equilibrium of the zero dynamics is locally asymptotically stable [23]. A linear-system analysis of FFL is given in [24], and its application to engineering structures is analyzed in [25]. FFL is mathematically equivalent to low-pass filtering a standard feedback linearization controller. However, unlike the standard feedback linearization, the controller only requires limited model information, specifically, knowledge of the vector relative degree and knowledge of the dynamic-inversion matrix, and makes the $\mathcal{L}_\infty$ of the command following error arbitrarily small despite the presence of unknown disturbances.

The main objective of this research paper is the applicability of filtered feedback linearization control approach in a heterogeneous traffic network. Heterogeneous traffic network has various forms of disturbances due the multiple types of vehicles with different characteristics. Also, it is almost impossible to measure all the disturbances in the traffic system and have a complete knowledge of the states of the system. Combination of FFL control approach and METANET macroscopic traffic model has the following benefits:

- Unlike the standard feedback linearization, the controller only requires limited model information, specifically, knowledge of the vector relative degree and knowledge of the dynamic-inversion matrix
- The controller has disturbance rejection for highly uncertain MIMO nonlinear subsystems that are potentially subject to unknown disturbance.
- METANET model is a second order macroscopic traffic model which help us to simulate all kinds of traffic conditions (Free-flow, Semi-congested, Congested) with prescribed characteristics (location, intensity, duration) which allow us to control the velocity of the traffic network as a feasible way of action in real world traffic network

The outline of this paper is as follows. Section 2 presents the model of a heterogeneous traffic network using the multi-class METANET model. Section 3 presents the basics of the FFL controller to maximize the mobility of the traffic network. Section 4 presents numerical results, and section 5 is the conclusion where we also discuss our future plans.

MACROSCOPIC DYNAMICS OF HETEROGENEOUS TRAFFIC NETWORK

Consider a non-signalized heterogeneous traffic network wherein the road is shared between the human-driven vehicles and autonomous vehicles. The road can be discretized into multiple sub-networks. We characterize sub-network $i \in \{1, 2, \cdots, n\}$ by its length ℓ_i, density of human-driven and autonomous vehicles ($k_{i,\mathrm{H}}, k_{i,\mathrm{A}}$), space mean speed of each class ($v_{i,\mathrm{H}}, v_{i,\mathrm{A}}$), and the total average flow rate Q_i. To determine the fundamental relation between the average flow(Q_i), density(k_i) and space mean speed v_i, we adopt a multi-class METANET model [21]. METANET is a second-order model in which considers the density and velocity of each vehicle class as traffic states. The control input in this model is considered as the suggested velocity for each type of vehicle class. Next, we are going to discuss the multi-class METANET model which contains the dynamic behavior of both human-driven and autonomous vehicles in a heterogeneous traffic network.

1. HETEROGENEOUS METANET MODEL

The multi-class METANET model is an extension of the well-known METANET model [26]. In this model, in cell $i \in \{1, \cdots, n\}$, for each class of vehicles, two set of fundamental diagrams is defined that describe the macroscopic behavior of autonomous and human-driven vehicles in a homogeneous (fully autonomous or fully human-driven) traffic network. Fig. 1.b demonstrates two fundamental diagrams wherein a higher free-flow speed ($v_{\mathrm{f,A}} \geq v_{\mathrm{f,H}}$), critical density ($k_{\mathrm{c,A}} \geq k_{\mathrm{c,H}}$), capacity ($C_{\mathrm{A}} \geq C_{\mathrm{H}}$) and jam density ($k_{\mathrm{J,A}} \geq k_{\mathrm{J,H}}$) is assumed for autonomous vehicles with respect to human-driven vehicles. In the multi-class METANET model, based on the fundamental diagram properties of each class of vehicles and their densities within the sub-network, the road is divided into two sections and it is assumed that a vehicle class constrains itself within the assigned fraction of the road [27]. Therefore, the road fractions for different classes of vehicles are positive values ($\alpha_{i,\mathrm{A}} > 0, \alpha_{i,\mathrm{H}} > 0$), and the sum of all fractions cannot exceed $\alpha_{i,\mathrm{A}} + \alpha_{\mathrm{H}} \leq 1$. To determine α_{A} and α_{H}, various approaches have been proposed. For instance, in [28], they calculated the road fraction by using

each class density. In [29], they took another approach in order to define the road fraction. They assumed an identical distance gap between different classes of vehicles in the traffic network to obtain the road fractions. However, in [30], they defined the road fractions by assuming that the distance gaps for all types of vehicles are proportional to the length of the vehicles. There was another method that was used by [21], to calculate the road fractions in which they equated the velocities of different classes of vehicles in the traffic network. In this paper, we also use a similar approach to calculate the space fractions for vehicles in the congested regime.

In this paper, according to different densities and their relative behavior in the traffic network, three traffic regimes are distinguished [21]: free-flow, semi-congested, congested (see Fig.1.a). These regimes are defined below. For all of these regimes, we assume that each vehicle class occupies the road optimally and never occupies more space than is necessary.

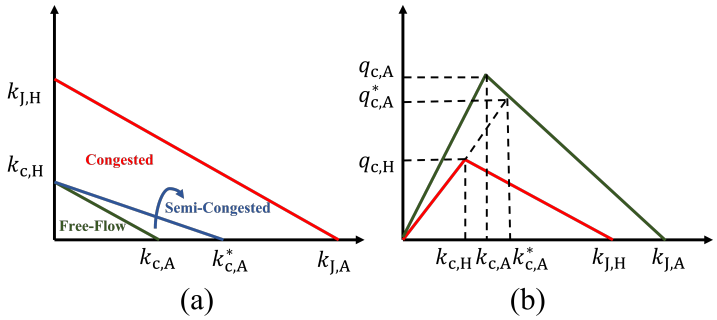

Figure 1: Three traffic regimes in the METANET model shown in MFD

Free-Flow Regime: The first possible traffic regime is that both human-driven and autonomous vehicles drive at their free-flow velocity. To this end, in the free-flow regime, it is assumed that density of each class of vehicles in the assigned space is less than or equal to the critical density of that class. In particular,

$$\frac{k_{i,\mathrm{H}}}{k_{\mathrm{c,H}}} + \frac{k_{i,\mathrm{A}}}{k_{\mathrm{c,A}}} \leq 1 \tag{1}$$

and the following sufficient and necessary condition is satisfied in free-flow regime:

$$\frac{k_{i,\mathrm{H}}}{\alpha_{i,\mathrm{H}}} \leq k_{\mathrm{c,H}}, \quad \frac{k_{i,\mathrm{A}}}{\alpha_{i,\mathrm{A}}} \leq k_{\mathrm{c,A}} \tag{2}$$

Therefore, it follows from equations (1 and (2) that space fractions of each vehicle class in the free-flow regime are:

$$\alpha_{i,\mathrm{H}} = \frac{k_{i,\mathrm{H}} k_{c,\mathrm{A}}}{k_{i,\mathrm{H}} k_{c,\mathrm{A}} + k_{i,\mathrm{A}} k_{c,\mathrm{H}}}, \alpha_{i,\mathrm{A}} = \frac{k_{i,\mathrm{A}} k_{c,\mathrm{H}}}{k_{i,\mathrm{A}} k_{c,\mathrm{H}} + k_{i,\mathrm{H}} k_{c,\mathrm{A}}} \tag{3}$$

Semi-Congested Regime: The second possible traffic regime is semi-congested where the vehicle class with a smaller free-flow velocity (i.e., human-driven) drive at the free-flow velocity but the other vehicle class with a larger free-flow velocity (i.e., autonomous vehicles) experience congestion and drive at a speed lower than its free-flow velocity. The important point in the semi-congested regime is that the velocity of autonomous class vehicles is still greater than or equal to the free-flow velocity of human-driven vehicles. This regime can be identified if the following constraint is satisfied:

$$\frac{k_{i,\mathrm{H}}}{k_{\mathrm{c,H}}} + \frac{k_{i,\mathrm{A}}}{k^*_{\mathrm{c,A}}} \leq 1 \tag{4}$$

where $k^*_{\mathrm{c,A}}$ is the "perceived" critical density of autonomous vehicles and is defined as:

$$k^*_{\mathrm{c,A}} = k_{\mathrm{c,A}} \left[-a_{\mathrm{m,A}} \ln \left(\frac{\mathrm{v_{f,H}}}{\mathrm{v_{f,A}}} \right) + 1 \right]^{\frac{1}{a_{\mathrm{m,A}}}} \tag{5}$$

Considering the optimal road use assumption, the space fraction of each class of vehicle in semi-congested regime is determined as:

$$\alpha_{i,\mathrm{A}} = \frac{k^*_{i,\mathrm{A}}}{k_{\mathrm{c,A}}}, \quad \alpha_{i,\mathrm{H}} = \frac{k_{i,\mathrm{H}}}{k_{\mathrm{c,H}}} \tag{6}$$

Congested Regime: The third possible traffic regime is that both human-driven and autonomous vehicles drive at a slower speed than the free-flow velocity. In a congested regime, autonomous and human-driven class vehicles both have the same velocity. The constraint of the congestion regime is the maximum density restriction.

$$\frac{k_{i,\mathrm{H}}}{k_{\mathrm{J,H}}} + \frac{k_{i,\mathrm{A}}}{k_{\mathrm{J,A}}} \leq 1 \tag{7}$$

The space fraction of each class of vehicle in semi-congested regime is determined as

$$V\Big(\frac{k_{i,\mathrm{H}}}{\alpha_{i,\mathrm{H}}}\Big) = V\Big(\frac{k_{i,\mathrm{A}}}{\alpha_{i,\mathrm{A}}}\Big), \quad \alpha_{i,\mathrm{A}} = \frac{A}{B}, \quad \alpha_{i,\mathrm{H}} + \alpha_{i,\mathrm{A}} = 1 \tag{8}$$

$$\begin{aligned} A = &\Big((k_{\mathrm{c,H}} - k_{\mathrm{J,H}}) k_{\mathrm{c,A}} v_{\mathrm{f,A}} \\ &- (k_{\mathrm{c,A}} - k_{\mathrm{J,A}}) k_{\mathrm{c,H}} v_{\mathrm{f,H}}\Big) k_{\mathrm{A}} k_{\mathrm{H}} \\ &+ (k_{\mathrm{c,A}} - k_{\mathrm{J,A}}) k_{\mathrm{c,H}} k_{\mathrm{J,H}} v_{\mathrm{f,H}}\ k_{\mathrm{A}} \\ B = &\ (k_{\mathrm{c,A}} - k_{\mathrm{J,A}}) k_{\mathrm{c,H}} k_{\mathrm{J,H}} v_{\mathrm{f,H}} k_{\mathrm{A}} \\ &+ (k_{\mathrm{c,H}} - k_{\mathrm{J,H}}) k_{\mathrm{c,A}} k_{\mathrm{J,A}} v_{\mathrm{f,A}} k_{\mathrm{H}} \end{aligned}$$

The total average flow relationship in a Macroscopic Fundamental Diagram (MFD) can be calculated through following equation:

$$Q_i = k_{i,\mathrm{H}} V\Big(\frac{k_{i,\mathrm{H}}}{\alpha_{i,\mathrm{H}}}\Big) + k_{i,\mathrm{A}} V\Big(\frac{k_{i,\mathrm{A}}}{\alpha_{i,\mathrm{A}}}\Big) \tag{9}$$

where Q_i is the total average flow which depends on the densities and average velocities of both autonomous and human-driven vehicles. Fig. 2 shows the average flow rate of the traffic network for a full spectrum of heterogeneity is shown.

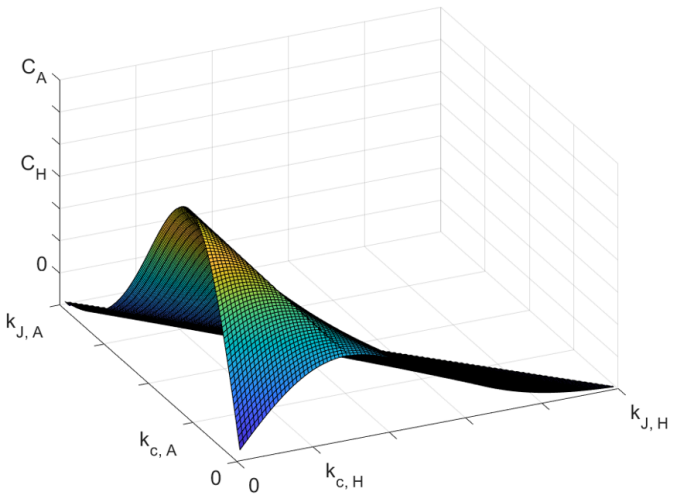

Figure 2: 3D Macroscopic Fundamental Diagram (MFD) for a full spectrum of heterogeneity. In fully autonomous traffic network, the maximum average flow rate C_A occurs at $k_{c,\mathrm{A}}$ and in fully human-driven traffic network, the maximum average flow C_H occurs at $k_{c,\mathrm{H}}$.

2. EQUATIONS OF MOTION

Consider a non-signalized heterogeneous traffic network. For a sub-network $i \in \{1, \cdots, n\}$, let $q_{i,\mathrm{A}}$ and $q_{i,\mathrm{H}}$ be outflow (number of autonomous and human-driven vehicles leaving the sub-network i to the adjacent sub-network $i+1$ and d_i be the uncontrolled traffic demand including the off-ramps and on-ramps. Also, consider ℓ as the length of the segment and γ as the number of the lanes in the segment. Then, the density of sub-network i is updated according to the conservation law [31]. Specifically,

$$k_{i,\mathrm{A}}(t+1) = k_{i,\mathrm{A}}(t) + \frac{T}{\ell_i \gamma_i}(q_{i-1,\mathrm{A}} - q_{i,\mathrm{A}} + d_{i,\mathrm{A}}) \quad (10a)$$

$$k_{i,\mathrm{H}}(t+1) = k_{i,\mathrm{H}}(t) + \frac{T}{\ell_i \gamma_i}(q_{i-1,\mathrm{H}} - q_{i,\mathrm{H}} + d_{i,\mathrm{H}}) \quad (10b)$$

Following the multi-class METANET model, the velocity of each class of vehicles can be described as

$$v_{i,\mathrm{A}}(t+1) = v_{i,\mathrm{A}}(t) + \frac{T}{\ell}\Big[v_{i,\mathrm{A}}(t)\Big(v_{i-1,\mathrm{A}}(t) - v_{i,\mathrm{A}}(t)\Big) - \frac{\gamma_{\mathrm{A}}}{\tau_{\mathrm{A}}}\frac{k_{i+1,\mathrm{A}}(t) - k_{i,\mathrm{A}}(t)}{k_{i,\mathrm{A}}(t) + k_{\mathrm{c,A}}\zeta_{\mathrm{A}}}\Big] + \frac{T}{\tau_{\mathrm{A}}}\Big(U_{i,\mathrm{A}}(t) - v_{i,\mathrm{A}}(t)\Big) \quad (11a)$$

$$v_{i,\mathrm{H}}(t+1) = v_{i,\mathrm{H}}(t) + \frac{T}{\ell}\Big[v_{i,\mathrm{H}}(t)\Big(v_{i-1,\mathrm{H}}(t) - v_{i,\mathrm{H}}(t)\Big) - \frac{\gamma_{\mathrm{H}}}{\tau_{\mathrm{H}}}\frac{k_{i+1,\mathrm{H}}(t) - k_{i,\mathrm{H}}(t)}{k_{i,\mathrm{H}}(t) + k_{\mathrm{c,H}}\zeta_{\mathrm{H}}}\Big] + \frac{T}{\tau_{\mathrm{H}}}\Big(U_{i,\mathrm{H}}(t) - v_{i,\mathrm{H}}(t)\Big) \quad (11b)$$

with

$$U_{i,\mathrm{A}} = (\beta_{i,\mathrm{A}}) v_{\mathrm{f,A}} \exp\left[\frac{-1}{a_{\mathrm{m,A}}}\left(\frac{k_{i,\mathrm{A}}(t)}{\alpha_{i,\mathrm{A}} k_{\mathrm{c,A}}}\right)^{a_{\mathrm{m,A}}}\right] \quad (12a)$$

$$U_{i,\mathrm{H}} = (\beta_{i,\mathrm{H}}) v_{\mathrm{f,H}} \exp\left[\frac{-1}{a_{\mathrm{m,H}}}\left(\frac{k_{i,\mathrm{H}}(t)}{\alpha_{i,\mathrm{H}} k_{\mathrm{c,H}}}\right)^{a_{\mathrm{m,H}}}\right] \quad (12b)$$

where $\beta_{i,\mathrm{A}}$ and $\beta_{i,\mathrm{H}}$ can considered as the control commands adjusting the suggested velocity to the autonomous vehicles and human-driven vehicles. According to Eqs.12a,12b, when $\beta_{i,\mathrm{H}} = \beta_{i,\mathrm{A}} = 1$, the traffic follows the regular MFD model and when $\beta_{i,\mathrm{H}} = \beta_{i,\mathrm{A}} = 0$, the controller is commanding vehicles to stop.

Finally, the origin outflow is calculated as [21]:

$$q_{0,\mathrm{A}}(t) = \min\left[d_{0,\mathrm{A}}(t) + \frac{\omega_{0,\mathrm{A}}(t)}{T}, \alpha_{1,\mathrm{A}} C_{0,\mathrm{A}} \kappa_{\mathrm{A}}\right] \quad (13a)$$

$$q_{0,\mathrm{H}}(t) = \min\left[d_{0,\mathrm{H}}(t) + \frac{\omega_{0,\mathrm{H}}(t)}{T}, \alpha_{1,\mathrm{H}} C_{0,\mathrm{H}} \kappa_{\mathrm{H}}\right] \quad (13b)$$

where $\kappa_{\mathrm{A}} = \left(\frac{k_{\mathrm{J,A}} - \frac{k_{1,\mathrm{A}}(t)}{\alpha_{1,\mathrm{A}}}}{k_{\mathrm{J,A}} - k_{\mathrm{c,A}}}\right)$, $\kappa_{\mathrm{H}} = \left(\frac{k_{\mathrm{J,H}} - \frac{k_{1,\mathrm{H}}(t)}{\alpha_{1,\mathrm{H}}}}{k_{\mathrm{J,H}} - k_{\mathrm{c,H}}}\right)$ and $C_{0,\mathrm{A}}$ and $C_{0,\mathrm{H}}$ are the theoretical maximum capacity of origin 0 for both types of vehicles. Also, $d_{0,\mathrm{A}}$ and $d_{0,\mathrm{H}}$ are the demand of autonomous and human-driven vehicles at origin 0.

For a traffic network consisting of n sub-network, by combining equations (10a)-(12b), the equations of motion can be expressed as

$$\dot{x} = \mathcal{F}(x) + \mathcal{G}(x)(u) + d \quad (14)$$

where $x = [x_1, \cdots, x_n]^{\mathrm{T}}$, $d = [d_1, \cdots, d_n]^{\mathrm{T}}$, $u = [\beta_{1,\mathrm{A}}, \beta_{1,\mathrm{H}}, \cdots, \beta_{n,\mathrm{A}}, \beta_{n,\mathrm{H}}]$, $\mathcal{F} = [f_1, \cdots, f_n]^{\mathrm{T}}$, $\mathcal{G} = [g_1, \cdots, g_n]^{\mathrm{T}}$. Here for $i \in \{1, \cdots, n\}$, $g_{i,\mathrm{A}} = v_{\mathrm{f,A}} \exp\left[\frac{-1}{a_{\mathrm{m,A}}}\left(\frac{k_{i,\mathrm{A}}(t)}{\alpha_{i,\mathrm{A}} k_{\mathrm{c,A}}}\right)^{a_{\mathrm{m,A}}}\right]$ and, $g_{i,\mathrm{H}} = v_{\mathrm{f,H}} \exp\left[\frac{-1}{a_{\mathrm{m,H}}}\left(\frac{k_{i,\mathrm{H}}(t)}{\alpha_{i,\mathrm{H}} k_{\mathrm{c,H}}}\right)^{a_{\mathrm{m,H}}}\right]$

TRAFFIC MANAGEMENT CONTROLLER

This section focuses on the design of a lower level of a hierarchical traffic management controller to improve the performance of a heterogeneous traffic network in terms of mobility. The filtered feedback linearization controller is utilized in the lower level and the description of its algorithm is given below.

1-FILTERED FEEDBACK LINEARIZATION

In the lower-level control, we employ a filtered feedback linearization approach to determine the required control command $\beta_{i,\mathrm{A}}$ and $\beta_{i,\mathrm{H}}$. We select filtered feedback linearization controller in the lower-level since this controller only requires limited model information, specifically, the system's relative degree and an estimate of the nonlinear extension of the high-frequency-gain matrix, and does not require any knowledge of the disturbance in the system [23–25, 32]. Furthermore, it can be shown that FFL is capable of the $\mathcal{L}_\infty$ of the command following error arbitrarily small despite the presence of unknown disturbances [32]. Below, we summarize the FFL control approach.

Considering $\mathcal{Y}_i = [k_{i,\mathrm{A}}, k_{i,\mathrm{H}}]^{\mathrm{T}}$, evaluating the second

derivative of $\mathcal{Y}$ yields

$$\begin{bmatrix}\ddot{k}_{i,\mathrm{A}}\\ \ddot{k}_{i,\mathrm{H}}\end{bmatrix} = \begin{bmatrix}\Psi_{i,\mathrm{A}}(x,\phi_d)\\ \Psi_{i,\mathrm{H}}(x,\phi_d)\end{bmatrix} + \Gamma_i(x_i)\begin{bmatrix}\beta_{i,\mathrm{A}}\\ \beta_{i,\mathrm{H}}\end{bmatrix} \tag{15}$$

where $\Gamma_i(x_i)$ is non-singular for $k_{i-1,\mathrm{A}} \in (0, k_{\mathrm{J,A}})$, $k_{i-1,\mathrm{H}} \in (0, k_{\mathrm{J,H}})$, $U_{i-1,\mathrm{A}} \in (0, v_{\mathrm{f,A}})$, $U_{i-1,\mathrm{H}} \in (0, v_{\mathrm{f,H}})$, $k_{i,\mathrm{A}} \in (0, k_{\mathrm{J,A}})$, $k_{i,\mathrm{H}} \in (0, k_{\mathrm{J,H}})$, $U_{i,\mathrm{A}} \in (0, v_{\mathrm{f,A}})$, $U_{i,\mathrm{H}} \in (0, v_{\mathrm{v,H}})$ and $\phi_d = [d, \dot{d}, \ddot{d}]^{\mathrm{T}}$.

Then, the control commands generated by the standard feedback linearization approach can be expressed as

$$\begin{bmatrix}\beta^*_{i,\mathrm{A}}\\ \\ \beta^*_{i,\mathrm{H}}\end{bmatrix} = -\Gamma_i^{-1}(X)\begin{bmatrix}\nu_{i,\mathrm{A}} + \Psi_{i,\mathrm{A}}\\ \nu_{i,\mathrm{H}} + \Psi_{i,\mathrm{H}}\end{bmatrix} \tag{16}$$

$$\nu_{i,\mathrm{A}} = \ddot{k}^*_{i,\mathrm{A}} + a_{i,1}(\dot{k}^*_{i,\mathrm{A}} - \dot{k}_{i,\mathrm{A}}) + a_{i,0}(k^*_{i,\mathrm{A}} - k_{i,\mathrm{A}}) \tag{17a}$$

$$\nu_{i,\mathrm{H}} = \ddot{k}^*_{i,\mathrm{H}} + a_{i,1}(\dot{k}^*_{i,\mathrm{H}} - \dot{k}_{i,\mathrm{H}}) + a_{i,0}(k^*_{i,\mathrm{H}} - k_{i,\mathrm{H}}) \tag{17b}$$

where $a_{i,0}$ and $a_{i,1}$ are constants. It follows from Eq. (16) that $\beta^*_{i,\mathrm{A}}, \beta^*_{i,\mathrm{H}}$ require the measurement of the disturbance d as well as knowledge of $\Psi_i(x, \phi_d)$ which may not be feasible in practice.

To this end, we determine the implementable control commands $\beta_{i,\mathrm{A}}, \beta_{i,\mathrm{AH}}$ by passing $\beta^*_{i,\mathrm{A}}, \beta^*_{i,\mathrm{H}}$ through a low-pass filter. Specifically, let $\beta_{i,\mathrm{A}}, \beta_{i,\mathrm{H}}$ satisfy

$$\eta_z(\mathbf{p})\beta_{i,\mathrm{A}} = \eta_z(0)\beta^*_{i,\mathrm{A}} \tag{18}$$

$$\eta_z(\mathbf{p})\beta_{i,\mathrm{H}} = \eta_z(0)\beta^*_{i,\mathrm{H}} \tag{19}$$

where $\mathbf{p} = d/dt$, and η_z is a real polynomial of order $\rho \geq 1$ whose coefficients depend on the real parameter $z > 0$. The required conditions and examples of $\eta_z(s)$ are addressed in [23]. For example, $\eta_z(s)$ can be a polynomial $\eta_z(s) = (s + z)^3$.

Substituting Eq. 15 into Eq. (16) and substituting this result into Eqs. (19)-(19), FFL controller is defined as

$$\begin{bmatrix}(\eta_z(\mathbf{p}) - \eta_z(0))\beta_{i,\mathrm{A}}\\ (\eta_z(\mathbf{p}) - \eta_z(0))\beta_{i,\mathrm{H}}\end{bmatrix} = \eta_z(0)\Gamma_i^{-1}\begin{bmatrix}\ddot{e}_{i,\mathrm{A}} + a_1\dot{e}_{i,\mathrm{A}} + a_0 e_{i,\mathrm{A}}\\ \ddot{e}_{i,\mathrm{H}} + a_1\dot{e}_{i,\mathrm{H}} + a_0 e_{i,\mathrm{H}}\end{bmatrix} \tag{20}$$

where $e_{i,\mathrm{A}} = k^*_{i,\mathrm{A}} - k_{i,\mathrm{A}}$ and $e_{i,\mathrm{H}} = k^*_{i,\mathrm{H}} - k_{i,\mathrm{H}}$

The controllers (16) and (20) are mathematically equivalent. However, unlike Eq. (16), the control (20) does not require measurement of d_i or Ψ_i. Properties of the lower-level closed-loop are addressed by [23]-Lemma 1. Specifically, it is shown that there exists $z_{\mathrm{s}} > z_0$ such that for $z > z_{\mathrm{s}}$, the control command given by Eq. (20) stabilizes the dynamic system and makes the tracking error arbitrarily small.

4. SIMULATION RESULTS

In this section, we present a case study to demonstrate the effectiveness of the proposed approach for improving the mobility of a heterogeneous traffic network. We compare the outcomes of the proposed control approach in two scenarios where the frequency of the low-pass filter is low and high. In this study, we considered a traffic network with 4 heterogeneous sub-networks consisting human-driven and autonomous vehicles. We used the I-485 N of Exit 28 traffic flow data which was reported in Tuesday 22 December 2020 to calibrate the model parameters and model the origin outflow in our simulation. The concentration is on eastbound PM peak hour of the highway which is between 4:30-5:30 PM. For both scenarios, the boundary sub-networks which set the demand and supply of the whole traffic system and the initial states are the same. I-485 inner highway has 4 lanes with the speed limit of 70 miles/hr. Since there is not enough information on the on-ramp and off-ramp flow rates according to the NCDOT report, we consider a disturbance to the total average flow rate of each sub-network to make the model more realistic $d_i = 250\sin(\omega.t)\frac{veh}{hr}$ for $i = 1, ..., 4$. The initial states for each sub-network is shown below in Table 1:

Sub-network	Density ($\frac{veh}{km.lane}$)	Velocity($\frac{km}{hr}$)
1	$k_{\mathrm{A}} = 35, k_{\mathrm{H}} = 20$	$v_{\mathrm{A}} = v_{\mathrm{H}} = 20$
2	$k_{\mathrm{A}} = 50, k_{\mathrm{H}} = 25$	$v_{\mathrm{A}} = v_{\mathrm{H}} = 20$
3	$k_{\mathrm{A}} = 75, k_{\mathrm{H}} = 10$	$v_{\mathrm{A}} = v_{\mathrm{H}} = 30$
4	$k_{\mathrm{A}} = 30, k_{\mathrm{H}} = 20$	$v_{\mathrm{A}} = v_{\mathrm{H}} = 18$
5	$k_{\mathrm{A}} = k_{\mathrm{H}} = 15$	$v_{\mathrm{A}} = 90, v_{\mathrm{H}} = 70$

Table 1: Initial States Values

The free-flow velocity of autonomous vehicles is considered as $v_{\mathrm{f,A}} = 90\frac{km}{hr}$, the jam density of the human-driven vehicles in each sub-network is $k_{\mathrm{J,H}} = 100\frac{veh}{km.lane}$, the jam density of the autonomous vehicles in each sub-network is $k_{\mathrm{J,A}} = 200\frac{veh}{km.lane}$, the length of each sub-network is considered as $\ell = 1$ km and there are 4 lanes $\gamma = 4$ in each sub-network. The METANET model parameters are shown in below in Table 2:

Model Parameters	AVs	HDVs
a_{m}	2.42	1.789
γ	$45\frac{km^2}{hr}$	$60\frac{km^2}{hr}$
ζ	$14\frac{veh}{km.hr}$	$10\frac{veh}{km.hr}$
τ	$12s$	$12s$

Table 2: METANET Model Parameters Values

Every 7 minutes, the higher level controller, sends the optimal density for both vehicle classes in each sub-network

to the lower level controller. For the first 7 minutes time period, the reference density for each sub-network shown in Table 3. After 7 minutes, the lower level controller, receives a new set of densities to follow.

Desired Density ($\frac{veh}{km.lane}$)		
Sub-network	$0-7mins$	$7-14mins$
1	$k_{\mathrm{A}}^{*}=28, k_{\mathrm{H}}^{*}=12$	$k_{\mathrm{A}}^{*}=31, k_{\mathrm{H}}^{*}=19$
2	$k_{\mathrm{A}}^{*}=30, k_{\mathrm{H}}^{*}=20$	$k_{\mathrm{A}}^{*}=25, k_{\mathrm{H}}^{*}=19$
3	$k_{\mathrm{A}}^{*}=38, k_{\mathrm{H}}^{*}=13$	$k_{\mathrm{A}}^{*}=30, k_{\mathrm{H}}^{*}=18$
4	$k_{\mathrm{A}}^{*}=24, k_{\mathrm{H}}^{*}=17$	$k_{\mathrm{A}}^{*}=25, k_{\mathrm{H}}^{*}=14$

Table 3: Desired densities of each class of vehicles in each sub-network during the simulation

The low-pass filter that we considered for the FFL controller is a polynomial as $\eta_z(s)=(s+z)^3$. In this paper, we compared the results for two different low-pass frequency values, $z=1$ and $z=100$. In Fig.3, the density of each vehicle class is shown for sub-networks 2 and 3 for both controller designs.

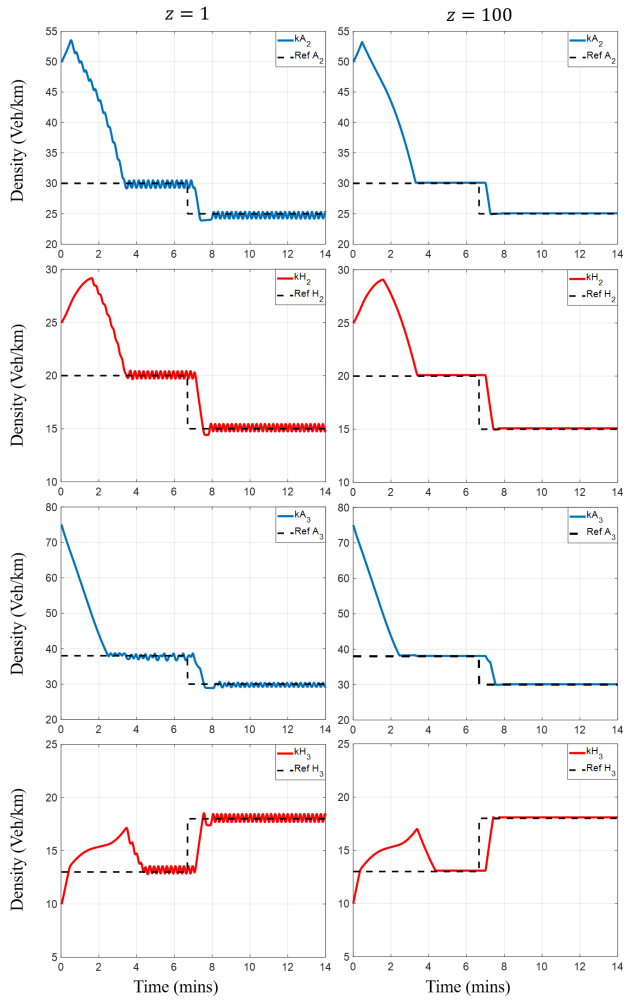

Figure 3: Density of autonomous and human driven vehicles for sub-networks 2 and 3 and their reference densities are shown.

As it can be seen in Fig.3, for $z=1$, we have an oscillation near the reference point but for $z=100$, the densities in each sub-network, can merge to the desired densities smoothly. In Fig.4, the velocities of both vehicle classes are shown for $z=1$ and $z=100$:

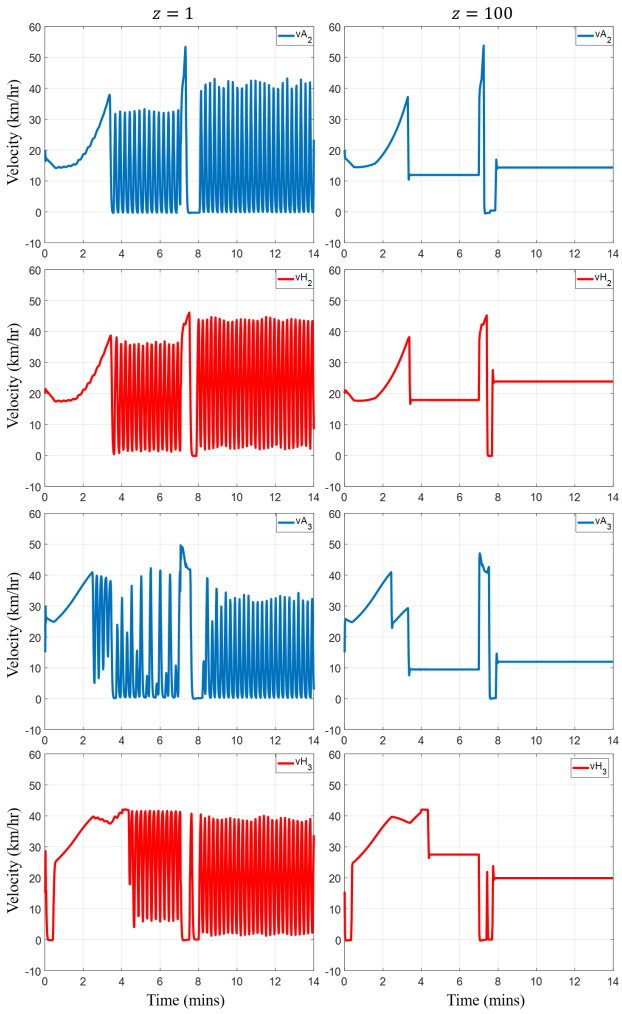

Figure 4: Velocity of autonomous and human-driven vehicles in sub-networks 2 and 3 are shown for both controller designs.

Fig.4 shows that with lower low-pass frequency in FFL controller, the oscillation for velocity of each vehicle class increases and it makes the traffic system unstable. For $z=100$, the velocities of both autonomous and human-driven vehicles change smoothly without any oscillation. Finally, Fig.5 shows the controller command (β_i) for each vehicle class in sub-networks 2 and 3. As it is shown, for $z=1$, the oscillation makes the traffic network unstable since it has drastic changes in a short time period. However, for $z=100$, the controller command perfectly controls the suggested velocity of each vehicle class so the sub-network can reach to the desired densities.

5. CONCLUSIONS

This paper focuses on modeling and controlling a non-signalized heterogeneous traffic network consisting of

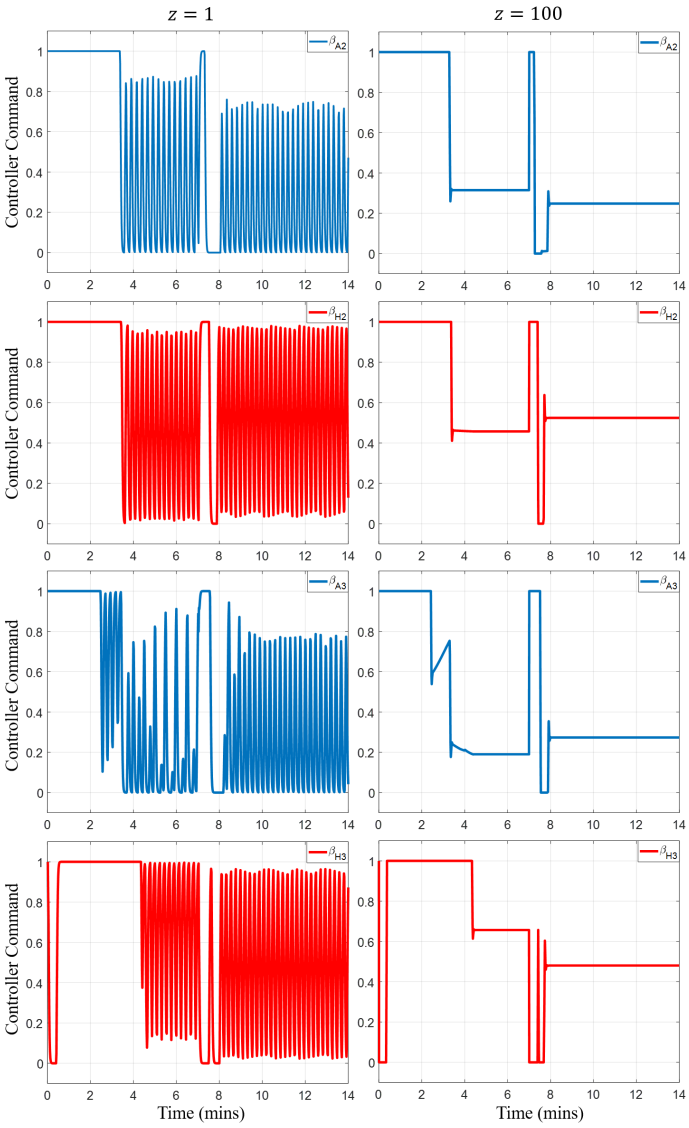

Figure 5: The FFL controller command for both autonomous and human-driven vehicles are shown. $\beta_i = 1$ is indicating that the traffic flow is following the MFD behavior and $\beta_i = 0$ indicates that the controller is commanding the vehicles to stop.

human-driven and autonomous vehicles. In this paper, the heterogeneity in the operational characteristics is considered. It is assumed that autonomous vehicles have a higher free-flow velocity and different model parameters compared to human-driven vehicles. We considered a two-level control structure in which the higher level, a decentralized control approach determines an optimal density of human and autonomous vehicles so that the average flow within a sub-network is maximized. At the lower level, a filtered feedback linearization controller is designed to determine the velocity of autonomous and human-driven vehicles such that the density of the autonomous and human-driven vehicles reaches the values set by the upper-level controller. In the future, we extend this case study considering the heterogeneity in the controllability of the two-class of vehicles. In particular, we consider to what extend the mobility of the traffic network can be improved if only autonomous vehicles can receive the commands sent by the higher-level controller. We further plan to validate our control approach with more sophisticated traffic simulators.

REFERENCES

[1] Graham Cookson and Bob Pishue. Inrix global traffic scorecard–appendices. *INRIX research*, 2017.

[2] Weili Sun, Jianfeng Zheng, and Henry X Liu. A capacity maximization scheme for intersection management with automated vehicles. *Transportation research procedia*, 23:121–136, 2017.

[3] Daniel A Lazar, Ramtin Pedarsani, Kabir Chandrasekher, and Dorsa Sadigh. Maximizing road capacity using cars that influence people. In *2018 IEEE Conference on Decision and Control (CDC)*, pages 1801–1808. IEEE, 2018.

[4] Catherine Ross and Subhrajit Guhathakurta. Autonomous vehicles and energy impacts: a scenario analysis. *Energy Procedia*, 143:47–52, 2017.

[5] Lanhang Ye and Toshiyuki Yamamoto. Modeling connected and autonomous vehicles in heterogeneous traffic flow. *Physica A: Statistical Mechanics and its Applications*, 490:269–277, 2018.

[6] Guni Sharon and Peter Stone. A protocol for mixed autonomous and human-operated vehicles at intersections. In *International Conference on Autonomous Agents and Multiagent Systems*, pages 151–167. Springer, 2017.

[7] Jian Wang, Srinivas Peeta, and Xiaozheng He. Multiclass traffic assignment model for mixed traffic flow of human-driven vehicles and connected and autonomous vehicles. *Transportation Research Part B: Methodological*, 126:139–168, 2019.

[8] Fangfang Zheng, Can Liu, Xiaobo Liu, Saif Eddin Jabari, and Liang Lu. Analyzing the impact of automated vehicles on uncertainty and stability of the mixed traffic flow. *Transportation research part C: emerging technologies*, 112:203–219, 2020.

[9] Negar Mehr and Roberto Horowitz. How will the presence of autonomous vehicles affect the equilibrium state of traffic networks? *IEEE Transactions on Control of Network Systems*, 7(1):96–105, 2019.

[10] Ajith Muralidharan and Roberto Horowitz. Computationally efficient model predictive control of freeway networks. *Transportation Research Part C: Emerging Technologies*, 58:532–553, 2015.

[11] Pouria Karimi Shahri, Amir H Ghasemi, and Vahid Izadi. Optimal lane management in heterogeneous traffic network using extremum seeking approach. Technical report, SAE Technical Paper, 2020.

[12] Ardalan Vahidi and Antonio Sciarretta. Energy saving potentials of connected and automated vehicles. *Transportation Research Part C: Emerging Technologies*, 95:822–843, 2018.

[13] Antonio Sciarretta and Ardalan Vahidi. Energy saving potentials of cavs. In *Energy-Efficient Driving of Road Vehicles*, pages 1–31. Springer, 2020.

[14] Jackeline Rios-Torres and Andreas A Malikopoulos. A survey on the coordination of connected and automated vehicles at intersections and merging at highway on-ramps. *IEEE Transactions on Intelligent Transportation Systems*, 18(5):1066–1077, 2016.

[15] Yu-Chiun Chiou, Chen-An Sun, and Chih-Wei Hsieh. A macro-micro model under mixed traffic flow conditions. *Journal of the Eastern Asia Society for Transportation Studies*, 11:1931–1944, 2015.

[16] Sasan Amini, Ilias Gerostathopoulos, and Christian Prehofer. Big data analytics architecture for real-time traffic control. In *2017 5th IEEE international conference on models and technologies for intelligent transportation systems (MT-ITS)*, pages 710–715. IEEE, 2017.

[17] RP Alvarez Gil, Zsolt Csaba Johanyák, Tamás Kovács, et al. Surrogate model based optimization of traffic lights cycles and green period ratios using microscopic simulation and fuzzy rule interpolation. *Int. J. Artif. Intell*, 16(1):20–40, 2018.

[18] Pouria Karimi Shahri, Shubhankar Chintamani Shindgikar, Baisravan HomChaudhuri, and Amir H Ghasemi. Optimal lane management in heterogeneous traffic network. In *Dynamic Systems and Control Conference*, volume 59162, page V003T18A003. American Society of Mechanical Engineers, 2019.

[19] Goof Sterk van de Weg, Hai L Vu, Andreas Hegyi, and Serge Paul Hoogendoorn. A hierarchical control framework for coordination of intersection signal timings in all traffic regimes. *IEEE Transactions on Intelligent Transportation Systems*, 20(5):1815–1827, 2018.

[20] Mohsen Ramezani, Jack Haddad, and Nikolas Geroliminis. Dynamics of heterogeneity in urban networks: aggregated traffic modeling and hierarchical control. *Transportation Research Part B: Methodological*, 74:1–19, 2015.

[21] Shuai Liu, Bart De Schutter, and Hans Hellendoorn. Model predictive traffic control based on a new multiclass metanet model. *IFAC Proceedings Volumes*, 47(3):8781–8786, 2014.

[22] Xu Wang, Derek Yin, and Tony Z Qiu. Applicability analysis of an extended metanet model in traffic-state prediction for congested freeway corridors. *Journal of Transportation Engineering, Part A: Systems*, 144(9):04018046, 2018.

[23] Jesse B Hoagg and TM Seigler. Filtered-dynamic-inversion control for unknown minimum-phase systems with unknown-and-unmeasured disturbances. *International Journal of Control*, 86(3):449–468, 2013.

[24] Jesse B Hoagg and TM Seigler. Decentralized filtered dynamic inversion for uncertain minimum-phase systems. *Automatica*, 61:192–200, 2015.

[25] Amir H Ghasemi. Slewing and vibration control of a single-link flexible manipulator using filtered feedback linearization. *Journal of Intelligent Material Systems and Structures*, 28(20):2887–2895, 2017.

[26] Markos Papageorgiou. *Applications of automatic control concepts to traffic flow modeling and control*. Springer, 1983.

[27] Steven Logghe. Dynamic modeling of heterogeneous vehicular traffic. *Faculty of Applied Science, Katholieke Universiteit Leuven, Leuven*, 2, 2003.

[28] Sylvie Benzoni-Gavage and Rinaldo M Colombo. An-populations model for traffic flow. *European Journal of Applied Mathematics*, 14(5):587–612, 2003.

[29] Stéphane Chanut and Christine Buisson. Macroscopic model and its numerical solution for two-flow mixed traffic with different speeds and lengths. *Transportation research record*, 1852(1):209–219, 2003.

[30] X Zotos, F Naef, and P Prelovsek. Transport and conservation laws. *Physical Review B*, 55(17):11029, 1997.

[31] Kanok Boriboonsomsin, Matthew J Barth, Weihua Zhu, and Alexander Vu. Eco-routing navigation system based on multisource historical and real-time traffic information. *IEEE Transactions on Intelligent Transportation Systems*, 13(4):1694–1704, 2012.

[32] Amir H Ghasemi, Jesse B Hoagg, and TM Seigler. Decentralized filtered feedback linearization for uncertain nonlinear systems. *International Journal of Robust and Nonlinear Control*, 28(4):1496–1506, 2018.